HHS Public Access

Author manuscript

Cell. Author manuscript; available in PMC 2017 May 19.

Published in final edited form as:

Cell. 2016 May 19; 165(5): 1209–1223. doi:10.1016/j.cell.2016.04.012.

Two Conserved Histone Demethylases Regulate Mitochondrial Stress-Induced Longevity

Carsten Merkwirth[1,2,3,6], **Virginija Jovaisaite**[4,6], **Jenni Durieux**[1,3], **Olli Matilainen**[4], **Sabine D. Jordan**[1,3,5], **Pedro M. Quiros**[4], **Kristan K. Steffen**[1,3], **Evan G. Williams**[4], **Laurent Mouchiroud**[4], **Sarah N. Uhlein**[1,3], **Virginia Murillo**[2], **Suzanne C. Wolff**[1,3], **Reuben J. Shaw**[2], **Johan Auwerx**[4,*], and **Andrew Dillin**[1,3,*]

Johan Auwerx: admin.auwerx@epfl.ch; Andrew Dillin: dillin@berkeley.edu

[1]Howard Hughes Medical Institute, Department of Molecular and Cell Biology, University of California, Berkeley, Berkeley, CA 94720, USA [2]The Glenn Center for Aging Research, The Salk Institute for Biological Studies, 10010 North Torrey Pines Road, La Jolla, CA 92037, USA [3]The Glenn Center for Aging Research, University of California, Berkeley, Berkeley, CA, 94720, USA [4]Laboratory of Integrative and Systems Physiology, Interfaculty Institute of Bioengineering, École Polytechnique Fédérale de Lausanne (EPFL), Lausanne 1015, Switzerland [5]The Scripps Research Institute, Department of Chemical Physiology, 10550 North Torrey Pines Road, La Jolla, CA 92037, USA

Summary

Across eukaryotic species, mild mitochondrial stress can have beneficial effects on the lifespan of organisms. Mitochondrial dysfunction activates an unfolded protein response (UPR^{mt}), a stress signaling mechanism designed to ensure mitochondrial homeostasis. Perturbation of mitochondria

*Co-corresponding author.

[6]Co-first author

Accession Numbers: RNA-sequencing data have been deposited in the Gene Expression Omnibus (GEO) database under accession number GSE78990.

Supplemental Information: Supplemental Information includes Extended Experimental Procedures, six Supplemental Figures, four Supplemental Tables and can be found with this article online at.

Author Contributions: C.M., V.J., J.A. and A.D. conceived the study and wrote the manuscript with input from all co-authors. C.M. performed *C. elegans* RNAi screens, lifespan assays, RNA-seq sample preparations, fluorescence microscopy, qRT-PCR experiments, immunoblots related to *jmjd-1.2*/PHF8 and analyzed data. V.J. performed RNA-seq analysis, *C. elegans* lifespan assays, fluorescence microscopy, qRT-PCR experiments and immunoblots related to *jmjd-3.1*/JMJD3 and analyzed data. J.D. generated transgenic *C. elegans* lines by microinjection. O.M. performed some of the *C. elegans* experiments and generated *jmjd-3.1* overexpressing *C. elegans* strains. S.D.J. performed qRT-PCR experiments and analyzed data. P.M.Q. performed mammalian microarray and ChIP-seq analyses. K.K.S. helped with the RNA-seq sample preparations and performed RNA-seq gene expression analysis. S.N.U. performed *C. elegans* crosses, backcrosses and strain integrations of *jmjd-1.2* overexpressing lines. E.G.W. performed initial bioinformatic analyses on BXD mouse tissues. L.M. and C.M. identified *jmjd-3.1* as a UPR^{mt} regulator in a screening campaign. V.M. conducted the *C. elegans* lifespan suppressor screen. S.C.W. conceived the high-throughput *C. elegans* RNAi screens and wrote the manuscript. R.J.S. provided intellectual input and supported the early phase of the project.

J.A. is the Nestlé Chair in Energy Metabolism at the EPFL and a cofounder of Mitobridge, Inc. and declares no financial interest related to this work. A.D. is a cofounder of Proteostasis Therapeutics, Inc. and Mitobridge, Inc. and declares no financial interest related to this work.

during larval development in *C. elegans* not only delays aging but also maintains UPR^{mt} signaling, suggesting an epigenetic mechanism that modulates both longevity and mitochondrial proteostasis throughout life. We identify the conserved histone lysine demethylases *jmjd-1.2*/PHF8 and *jmjd-3.1*/JMJD3 as positive regulators of lifespan in response to mitochondrial dysfunction across species. Reduction-of-function of the demethylases potently suppresses longevity and UPR^{mt} induction while gain-of-function is sufficient to extend lifespan in an UPR^{mt}-dependent manner. A systems genetics approach in the BXD mouse reference population further indicates conserved roles of the mammalian orthologs in longevity and UPR^{mt} signaling. These findings illustrate an evolutionary conserved epigenetic mechanism that determines the rate of aging downstream of mitochondrial perturbations.

Introduction

Aging is a deleterious and complex process characterized by the progressive decline of cellular and organismal homeostasis amid constantly increasing levels of entropy (Kirkwood, 2005) and represents the primary risk factor in major human pathologies including cancer, diabetes, cardiovascular disorders, and neurodegenerative diseases (Lopez-Otin et al., 2013). Aging, however, is not only a response to experiences incurred toward the end of an organism's life: it is shaped and determined by experiences that have accumulated from the earliest stages of development, and even during the generations that came before it. The organism's perpetuation of historic cues – how its patterns of gene expression change and become cemented in response to stresses that may have occurred long in the past or in parental populations – have proven to significantly affect long-term health and longevity, the mechanistic details of which are only beginning to emerge. It is thus that we now know, for example, that the transgenerational inheritance of chromatin marks can increase lifespan for multiple generations in *C. elegans* (Greer et al., 2010; Han and Brunet, 2012; Lopez-Otin et al., 2013; Rando and Chang, 2012) underscoring the importance of understanding not only the genetic but also the epigenetic contributions to the complex and disordered aging process.

One of the most dramatic examples in which early events have effects on longevity is found in the nematode *C. elegans*, in which mitochondrial stress during development can cause nearly a doubling of the animal's lifespan (Dillin et al., 2002a). The timing and degree of mitochondrial dysfunction is highly selective: it must occur during a specific L3/L4 larval transition in order to cause lifespan extension, a time during which a heavy amount of germline-specific mitochondrial biogenesis also occurs (Rea et al., 2007; Tsang and Lemire, 2002). In contrast, mitochondrial dysfunction that is too severe or which is implemented too early or late can have a negative effect on lifespan. In many cases, titrating a level of dysfunction is absolutely required in order to observe an extension of lifespan (Rea et al., 2007). Longevity caused by mitochondrial dysfunction also often fails to generate universal health benefits, as organisms may live longer but exhibit developmental delay and a drastic reduction in reproductive fitness (Dillin et al., 2002a; Lee et al., 2003). These effects are surprisingly conserved: in yeast, flies, and mice, mitochondrial dysfunction can delay the aging process (Copeland et al., 2009; Dell'agnello et al., 2007; Dillin et al., 2002a; Feng et al., 2001; Kirchman et al., 1999; Lee et al., 2003; Liu et al., 2005), but, when occurring later

in life, has deleterious effects and is associated with age-onset neurodegenerative diseases, directly contributing to their pathologies (Schon and Przedborski, 2011).

Within mitochondria, intricate surveillance systems monitor the quality of existing and newly synthesized mitochondrial proteins to ensure mitochondrial homeostasis (Baker et al., 2011). The mitochondrial unfolded protein response (UPR^{mt}) consists of a signaling cascade that results in upregulation of nuclear-encoded genes to alleviate the stress sensed in mitochondria. Perception of misfolding in mitochondria requires the protease ClpP, which generates a mitochondrial derived signal to activate downstream genes (Haynes et al., 2007). ClpP triggers the activation of the ubiquitin-like protein UBL-5, which acts as a coactivator of the transcription factor DVE-1. UBL-5 and DVE-1 respond to mitochondrial perturbation to increase expression of mitochondrial chaperones, including *hsp-6* and *hsp-60* (Benedetti et al., 2006). In parallel, the bZIP transcription factor ATFS-1 coordinates a wide cellular response to mitochondrial stress (Nargund et al., 2012, 2015).

Previously, several genes characterized for their role in the regulation of the UPR^{mt} were identified as specific requirements for the long lifespan of animals with reduced mitochondrial function (Durieux et al., 2011; Houtkooper et al., 2013). The requirements for these genes in electron transport chain (ETC)-mediated longevity suggested that the function of the UPR^{mt} might have a beneficial effect on the organism and was required to maintain the longer lifespans in the mitochondrial mutants. In this model, mitochondrial dysfunction early in development was capable of imposing a mild, hormetic stress that could remodel gene expression patterns, perpetuating a beneficial effect long into adulthood (Durieux et al., 2011). In keeping with this hypothesis, induction of the UPR^{mt} during early larval stages persists long into adulthood, suggesting that the animal may possess an epigenetic mechanism to maintain the activation of stress responses and ensure increased resistance to future mitochondrial insults (Durieux et al., 2011). In yeast, mitochondrial stress generated by reactive oxygen species (ROS) causes an epigenetic remodeling that extends lifespan (Schroeder et al., 2013), and forced expression of UPR^{mt} genes in *Drosophila* is sufficient to preserve mitochondrial function (Owusu-Ansah et al., 2013).

In this study we identify two conserved histone lysine demethylases as regulators of the ETC longevity pathway. Using RNAi-based screens in *C. elegans*, we isolated the conserved histone demethylases *jmjd-1.2* and *jmjd-3.1* as potent suppressors of longevity in response to mitochondrial perturbations. We demonstrate that both *jmjd-1.2* and *jmjd-3.1* are necessary and sufficient for activation of the UPR^{mt} in *C. elegans*. Moreover, our experiments identify *jmjd-1.2* and *jmjd-3.1* as positive regulators of a longevity response that genetically requires UPR^{mt} signaling. Using transcriptome analysis, we demonstrate that *jmjd-1.2* and *jmjd-3.1* coordinate the transcriptional response to mitochondrial stress. Furthermore, using a systems genetics approach, we find that the mammalian orthologs exhibit positive genetic correlations with UPR^{mt} core components in the BXD mouse genetic reference population (Andreux et al., 2012; Wu et al., 2014). Together, these data reveal a conserved epigenetic mechanism that determines longevity and stress signaling in response to mitochondrial dysfunction.

Results

Mitochondrial ETC-Mediated Longevity Requires the Histone Lysine Demethylases *jmjd-1.2* and *jmjd-3.1*

We performed an RNAi-based screen to identify genes specifically required for the ETC-mediated longevity in *C. elegans*. Through these analyses, we identified a putative histone lysine demethylase of the JumonjiC (JmjC)-domain-containing protein family, *jmjd-1.2 (F29B9.2)*, (Kooistra and Helin, 2012), as a potent suppressor of the ETC longevity pathway (Figure 1A and Table S1). We hypothesized that other JmjC domain containing demethylases may have similar effects on the regulation of lifespan. From the JmjC orthologs found in *C. elegans*, we identified a second histone lysine demethylase, *jmjd-3.1 (F18E9.5)*, that was also an effective suppressor of ETC-mediated longevity (Figure 1B and Table S1). In their roles as demethylases, *jmjd-1.2* and *jmjd-3.1* have both distinct and overlapping specificity for histone modifications, most notably against H3K27me2/3 (Agger et al., 2007; Kleine-Kohlbrecher et al., 2010). We found that both *jmjd-1.2* and *jmjd-3.1* were required for the extended lifespan caused by point mutation in the Rieske iron-sulfur protein (complex III), *isp-1(qm150)* (Feng et al., 2001) (Figures 1C, D). Downregulation of the closely related H3K27me2/3 demethylases *jmjd-3.2*, *jmjd-3.3* and *utx-1*, however, did not significantly affect lifespan extension by *cco-1* RNAi (Figure S1A), highlighting a specific role of *jmjd-1.2* and *jmjd-3.1* for ETC-mediated longevity.

Next, we assessed whether *jmjd-1.2* and *jmjd-3.1* were specific to lifespan extension in response to mitochondrial perturbation. The mitochondrial ETC longevity pathway acts in parallel to several other lifespan extending paradigms, including the insulin/IGF longevity response (Kenyon et al., 1993), dietary restriction (DR) (Lakowski and Hekimi, 1998), and germline-mediated longevity (Hsin and Kenyon, 1999). Neither *jmjd-1.2* nor *jmjd-3.1* downregulation altered longevity of dietary restricted *eat-2(ad1116)* animals (Figures 1E, F). We further found that *jmjd-1.2* had no effect on the lifespan of animals in which stress responses of the ER or cytosol were constitutively activated (Baird et al., 2014; Taylor and Dillin, 2013) (Figures S1B-D) while transcription factors FoxO/*daf-16* and FoxA/*pha-4* successfully suppressed lifespan in our analyses (Figures 1E-H, Table S1). In contrast, while *jmjd-1.2* RNAi did not affect the extended longevity seen in *daf-2(e1370)* mutant animals or germline deficient *glp-1(e2141)* animals (Figures 1G, S1B), we observed that the long lifespan *daf-2(e1370)* mutant worms depended on *jmjd-3.1*, albeit partially (Figure 1H). Recently *jmjd-3.1* was also reported to be required for the lifespan extension of germline-deficient *glp-1* animals (Labbadia and Morimoto, 2015). Collectively, these data indicate that while *jmjd-3.1* is involved in several lifespan extension paradigms, both histone demethylases are required for ETC-mediated longevity.

Overlapping Temporal Requirements of JmjC Demethylase Activity and ETC-Mediated Longevity

One of the most remarkable features of ETC-mediated longevity in *C. elegans* lies in its precise temporal requirements: Reduction of ETC function during a narrow window of development is sufficient to extend lifespan throughout life (Dillin et al., 2002a; Rea et al., 2007). In contrast, loss of ETC function in adulthood is sufficient to reduce ATP production

but can no longer affect lifespan. We reasoned that the activity of histone demethylases might be required during development and therefore performed RNAi shifting experiments in which we reduced ETC activity during development and restored them during adulthood by shifting young adults to *Dicer (dcr-1)* RNAi to inhibit the RNAi machinery (Dillin et al., 2002a, 2002b). We found that reduction of *jmjd-1.2* during larval development was sufficient to block *cco-1* mediated longevity (Figure S1E). *jmjd-1.2* RNAi during adulthood, in contrast, reduced *cco-1* lifespan partially (Figure S1F). *jmjd-3.1* was partially required for *cco-1* mediated longevity during larval development but had only a minor effect during adulthood (Figures S1G, H). These data suggest that both *jmjd-1.2* and *jmjd-3.1* are required for an initial response to ETC deficiency during development that is maintained into adulthood.

JMJD-1.2 and JMJD-3.1 Regulate the Mitochondrial Unfolded Protein Response (UPR^{mt})

Previously, the UPR^{mt} was found to be required for the extended longevity of mitochondrial mutants (Durieux et al., 2011). We therefore asked whether *jmjd-1.2* and *jmjd-3.1* had any effect on the induction of the UPR^{mt} in *C. elegans*. In these analyses, *cco-1* RNAi was used as a potent inducer of both *hsp-6* and *hsp-60* endogenous transcripts, robustly turning on the transcriptional *hsp-6p::gfp* reporter (Yoneda et al., 2004). As reported, *cco-1* mediated UPR^{mt} activation required the ClpP protease *clpp-1* and the homeodomain transcription factor *dve-1* (Haynes et al., 2007) (Figures 2A and S2B). Similarly, RNAi of either *jmjd-1.2* or *jmjd-3.1* suppressed the *hsp-6p::gfp* reporter activation elicited by *cco-1* (Durieux et al., 2011) (Figures 2A and S2A), *spg-7* (Yoneda et al., 2004) (Figures 2B and S2C) or *mrps-5* (Houtkooper et al., 2013) knockdowns (Figure S2D).

We tested additional JmjC-containing proteins for their effects on UPR^{mt} following mitochondrial stress (Figure S2A). Interestingly, RNAi against the H3K27 demethylase family members *jmjd-3.2*, *jmjd-3.3* and *utx-1* also substantially decreased UPR^{mt} activation, while other JmjC-domain containing demethylases had no significant effect on UPR^{mt} activation (Figures 2B, S2A). As an alternative approach, we used the H3K27 demethylase inhibitor GSK-J4 (Heinemann et al., 2014) to examine potential activity towards UPR^{mt} induction. GSK-J4 treatment of *hsp-6p::gfp* reporter animals grown on *mrps-5* RNAi suppressed UPR^{mt} activation (Figure S2E) indicating that H3K27 demethylase activity was required for the perpetuation of mitochondrial stress signaling. As H3K27 methylation can be established by the Polycomb repressive complex 2 (PRC2) in *C. elegans* (Bender et al., 2004), we asked whether reduction of polycomb components is sufficient to trigger the UPR^{mt}. However, knockdown of individual PRC2 components *mes-2*, *mes-3* and *mes-6* in *C. elegans* did not activate UPR^{mt} signaling (Figure S2F).

We next examined a potential contribution of *jmjd-1.2* and *jmjd-3.1* on additional cellular stress responses including the unfolded protein response of the endoplasmic reticulum (UPR^{er}) (Walter and Ron, 2011) and the cytosolic heat shock response (HSR) (Morimoto, 2011). RNAi against *jmjd-1.2* did not affect induction of UPR^{er} target genes, including the ER chaperone BiP (*hsp-4*), in response to UPR^{er} stimulation with tunicamycin (Figures 2C, S3A). In contrast, *jmjd-3.1* RNAi revealed minor but statistically significant effects on several UPR^{er} target genes, which became evident only upon monitoring gene expression

independent of the *hsp-4p::gfp* reporter (Figure 2D, S3B), consistent with recent findings (Labbadia and Morimoto, 2015). Moreover, RNAi against *jmjd-1.2* or *jmjd-3.1* did not affect the heat shock-induced expression of the HSR chaperone *hsp-16.2* (Figures 2E, F; S3C, D). Finally, *jmjd-1.2* and *jmjd-3.1* had no effect on the expression of the antioxidant enzyme *sod-3*, which is induced by reduced insulin/IGF-1 signaling (Figures 2G, H). Collectively, these data indicate that *jmjd-1.2* specifically modulates the UPR^{mt}, while *jmjd-3.1* appears to be moderately involved in the transcriptional response to ER stress.

Overexpression of *jmjd-1.2* or *jmjd-3.1* is Sufficient for Lifespan Extension and UPR^{mt} Induction

The results of the previous experiments indicated that both *jmjd-1.2* and *jmjd-3.1* were required for ETC-mediated longevity and UPR^{mt} induction. We next tested their sufficiency to extend lifespan and increase mitochondrial stress signaling. We generated transgenic strains expressing *jmjd-1.2* under control of the ubiquitous *sur-5* promoter and monitored lifespan. For control, we generated an enzymatically inactive version of *jmjd-1.2* that harbors a point mutation in the catalytic histidine of the JmjC domain (*jmjd-1.2^{H508A}*). *jmjd-1.2* overexpression significantly increased longevity when compared to wild type animals (Figure 3A), while the catalytically-inactive *jmjd-1.2^{H508A}* had no effect (Figure S4A). We also generated strains overexpressing *jmjd-3.1* under the control of its endogenous promoter (*jmjd-3.1p::jmjd-3.1*) and found these animals to be long-lived (Figure 3B), in agreement with previous reports (Labbadia and Morimoto, 2015).

Intriguingly, overexpression of either *jmjd-1.2* or *jmjd-3.1* was sufficient to induce the UPR^{mt} (Figures 3C-F). To identify the tissues in which expression was required, we generated transgenic strains expressing *jmjd-1.2* in either neurons or the intestine. Neuronal overexpression of *jmjd-1.2* was sufficient for lifespan extension and UPR^{mt} activation, while expression in the intestine did not (Figures 3G, H, S4B). Similarly, overexpression of the catalytically inactive *jmjd-1.2^{H508A}* variant failed to activate the UPR^{mt} (Figure S4B). Moreover, *jmjd-1.2* overexpression had no effect on mRNAs levels of UPR^{er} and HSR target genes indicating that *jmjd-1.2* selectively modulates the UPR^{mt} (Figures S4C, D). *jmjd-3.1* overexpression, however, lead to a significant increase in expression of some UPR^{er} target genes, but not of the HSR (Figures S4E, F).

The UPR^{mt} Is a Genetic Requirement for JmjC demethylase-mediated Longevity

The ubiquitin-like protein UBL-5 is required for increased longevity of the ETC mutant *isp-1(qm150)* (Durieux et al., 2011) (Figure S5A). Therefore, we tested whether the long lifespan of *jmjd-1.2* and *jmjd-3.1* overexpressing animals depended upon *ubl-5*. Intriguingly, *ubl-5* RNAi fully suppressed increased longevity of both *jmjd-1.2* and *jmjd-3.1*, as well as neuron-specific *jmjd-1.2* overexpressing animals (Figures 4A-C). Notably, *ubl-5* was not required for increased longevity of animals ubiquitously expressing heat shock factor-1 (HSF-1) (Baird et al., 2014) (Figure S5B) and had no effect on wild type lifespan (Durieux et al., 2011). These data strongly suggest that the UPR^{mt} is an essential and specific requirement in H3K27 demethylase *gain-of-function* models.

Since both *jmjd-1.2* and *jmjd-3.1* overexpression induced the UPR^{mt}, we also tested the requirement of the UPR^{mt} core components *clpp-1* and *atfs-1* for UPR^{mt} activation in response to demethylase overexpression. RNAi against *atfs-1* and *clpp-1* in strains overexpressing *jmjd-1.2* or *jmjd-3.1* efficiently abrogated UPR^{mt} signaling, suggesting that *jmjd-1.2* and *jmjd-3.1* function upstream of the core transcriptional UPR^{mt} machinery in *C. elegans* (Figures 4D-I).

JMJD-1.2 and JMJD-3.1 Overexpression Recapitulates the Transcriptional Response to Mitochondrial Stress—To understand the molecular mechanisms that underlie the extended longevity in response to mitochondrial ETC perturbation and histone demethylase overexpression on a whole genome level, we performed RNA-seq analysis of strains ubiquitously overexpressing *jmjd-3.1* or *jmjd-1.2*, or neuronally-expressed *jmjd-1.2*, and compared them to *cco-1* RNAi treated animals. Our analysis identified ~3,000-7,500 differentially expressed genes (DEGs) in each condition (adjusted p-value < 0.05), with the greatest number of changes observed in the *jmjd-3.1p::jmjd-3.1* strain (Figure 5A). Strikingly, almost half the genes differentially expressed upon *cco-1* RNAi treatment (1405/2979) were also significantly differentially expressed in all three demethylase overexpression strains, and 84% (2505/2979) were in common with at least one of the examined overexpression strains (Figure 5A). Among the overlapping DEGs, 99% (1385/1405) of gene expression changes go in the same direction in all 4 conditions (Figure 5E). These data indicate that an overwhelming majority of the gene expression changes induced by *cco-1* RNAi are recapitulated by overexpression of *jmjd-1.2* or *jmjd-3.1*. Furthermore, an examination of all nine JmjC-domain encoding genes revealed that *jmjd-1.2* and *jmjd-3.1* were specifically upregulated in response to *cco-1* RNAi treatment (Figure 5B). These data place *jmjd-1.2* and *jmjd-3.1* downstream of mitochondrial stress and support a model in which a majority of the transcriptional response to mitochondrial stress is mediated by *jmjd-1.2* and *jmjd-3.1*.

The 1405 overlapping genes were subjected to Gene Ontology (GO) analysis using the DAVID database (Huang et al., 2009). Among the upregulated genes, signaling and cell communication related terms were enriched (Figure 5D). Importantly, larval development and growth, as well as multiple protein processing pathways, such as translation and proteasome were extensively downregulated, consistent with global remodeling of the proteome in response to stress (Figure 5D). Whereas the majority of mitochondrial genes were significantly reduced in all examined conditions (Figure 5F, G), many of the UPR^{mt} components, such as the chaperone *hsp-6*, the proteases *ymel-1* and *spg-7* as well as the transcriptional regulator *dve-1* were induced (Figure 5C). Remarkably, OXPHOS genes in *jmjd-1.2* and *jmjd-3.1* overexpression strains were downregulated to a similar extent as in *cco-1* RNAi treated animals (Figure 5G). Surprisingly, there were only a few OXPHOS components that were significantly upregulated in all conditions, specifically *cyc-1* from complex III and mtDNA encoded *nduo-2*, *nduo-4* and *nduo-5*. Intriguingly, this finding is reminiscent of mito-nuclear protein imbalance, a phenomenon of contrasting expression between nuclear- and mtDNA encoded OXPHOS components which tightly couples UPR^{mt} activation with longevity across organisms (Houtkooper et al., 2013).

Mammalian PHF8 and JMJD3 Correlate with Lifespan and UPR^{mt} Activation

To assess the potential roles of *jmjd-1.2* and *jmjd-3.1* in regulating UPR^{mt} and longevity in mammals, we investigated their murine homologs *Phf8* and *Jmjd3*, respectively, in the GeneNetwork database (www.genenetwork.org), which contains a vast collection of clinical and molecular (transcript and protein expression) phenotypes from the BXD mouse genetic reference panel (GRP) (Andreux et al., 2012; Wu et al., 2014). Importantly, variations within these datasets reflect mild, natural variations in gene expression patterns found in isogenic populations and are not reliant upon more deleterious genetic manipulations of mitochondrial function.

Both the transcripts for *Phf8* and *Jmjd3* showed high levels of variability in expression across the tissues and strains examined (Figure 6A). In tissue-specific datasets, natural variations in *Phf8* expression in the hypothalamus, spleen, and amygdala positively correlated with *Jmjd3* expression (Figure 6B), suggesting a correlative genetic interaction between the two enzymes. Importantly, expression levels of both histone demethylases were also positively correlated with UPR^{mt} related genes, including *Hspd1* (encoding the mitochondrial chaperone HSP60), *Satb1*, *Satb2* (orthologs of the *C. elegans* UPR^{mt} regulator *dve-1*), *Abcb10* (ortholog of the mitochondrial peptide exporter *haf-1*) (Haynes et al., 2010) and *Ubl5* (ortholog of *ubl-5*) across an array of tissues (Figures 6C, D). The strongest associations were observed in the hypothalamus, in which UPR^{mt} related genes in addition to *Phf8* and *Jmjd3* formed a connected correlation network (Figure 6E). In accordance with the impact of *jmjd-1.2* and *jmjd-3.1* on lifespan regulation in *C. elegans*, we observed correlations between *Phf8* and *Jmjd3* expression and lifespan in the spleen and hypothalamus or pituitary and adrenal glands of mice, respectively (Figures 6F, G).

Across strains expressing variable levels of *Phf8* mRNA, using immunoblotting, we found a correlative change of PHF8 protein, which was paralleled by a reduction of global H3K27me2 levels (Figure 7A). Increased PHF8 protein levels were also associated with higher abundance of UPR^{mt} marker proteins, such as the chaperones mtHSP70 and HSP60 (Figure 7B), reminiscent of the transcript correlations (Figure 6C). Similarly, higher JMJD3 levels were associated with an increase of HSP60 protein (Figure 7C).

We hypothesized that a relationship between the expression of markers of UPR^{mt}, *Phf8*, and *Jmjd3* also might be detectable in mammalian *Jmjd3 loss-of-function* experiments, which have been published previously (GEO datasets GSE40332, GSE56696) (Ntziachristos et al., 2014). Consistent with our prediction, in *Jmjd3* knockout mouse embryos (GSE40332), the expression of various UPR^{mt} related transcripts was decreased (Figure 7D). Likewise, knockdown of JMJD3 by shRNA in two human T-cell lymphoma cell lines (CUTLL1 and CEM) decreased the expression levels of multiple transcripts related to the UPR^{mt} (Figure 7E). Similarly, treatment of CUTLL1 cell line with the H3K27 demethylase inhibitor GSK-J4 (GSE56696) (Ntziachristos et al., 2014) also decreased the levels of multiple UPR^{mt} transcripts in a time-dependent fashion (Figure 7F). Overall, these data in both the murine GRP, mice with *loss-of-function* alleles, or cell lines with modified levels or activity of PHF8 and/or JMJD3 collectively suggest that expression levels of these demethylases positively correlate with UPR^{mt} expression.

Finally, we examined ChIP-seq analysis of CUTLL1 cells treated with shJMJD3 (GSE56696) for evidence of direct JmjC regulation of chromatin at coding regions of UPR^{mt} target genes. In these analyses, we found that H3K27me3 enrichment on *HSPD1*, *HSPE1*, and *SATB1* genes was increased upon JMJD3 knockdown (Figure 7G), indicating that the repressive H3K27me3 mark may be actively removed from the coding regions of these genes by JMJD3, thereby allowing for their expression. In another independent ChIP-seq dataset (GSE20725) (Fortschegger et al., 2010), PHF8 was found to bind to coding regions of UPR^{mt} genes *HSPD1*, *HSPE1* and *UBL5* in both HeLa and 293T cells (Figure 7H).

In addition to these *in silico* analyses, we examined H3K27me3 occupancy at coding regions of UPR^{mt} regulators during mitochondrial stress in larval stage *C. elegans* by ChIP-qRT-PCR. We observed a substantial decrease in H3K27me3 abundance on *hsp-6*, *clpp-1* and *atfs-1* genes upon *cco-1* RNAi during early larval development (Figure 7I). Taken together, these data suggest that PHF8 and JMJD3 may be conserved positive regulators of UPR^{mt} and lifespan from *C. elegans* to mammals, through the modulation of the H3K27 methylation status at coding regions of key UPR^{mt} genes.

Discussion

The distinct timing requirements of lifespan extension due to mild mitochondrial dysfunction during larval development led to the early proposal of an epigenetic mechanism that determines ETC-mediated longevity of *C. elegans* (Dillin et al., 2002a; Durieux et al., 2011). Remarkably, the discovery that the UPR^{mt} is not only a genetic requirement but also shares these overlapping timing requirements with ETC-mediated longevity reinforces the idea that primary mitochondrial perturbations establish an epigenetic memory which sets the rate of aging of the entire organism and protects its mitochondrial proteome from future insults (Durieux et al., 2011). The identification of *jmjd-1.2/PHF8* and *jmjd-3.1/JMJD3* provides a molecular explanation for these observations and suggests the epigenetic regulation of transcriptional outputs during mitochondrial stress. We find *jmjd-1.2* to be not only necessary and specific, but also sufficient for both induction of the UPR^{mt} and extension of lifespan. *jmjd-3.1* is also necessary and sufficient for UPR^{mt} induction and lifespan extension, but has overlapping roles in ER stress regulation (Labbadia and Morimoto, 2015).

The two histone demethylases differ in their substrate specificity: While *jmjd-3.1*/JMJD3 is associated with the removal of H3K27me2/3 epigenetic marks (Agger et al., 2007), *jmjd-1.2*/PHF8 has activity towards a wider range of substrates, including H3K9me1/2, H3K27me2 and H4K20me1 (Feng et al., 2010; Fortschegger et al., 2010; Kleine-Kohlbrecher et al., 2010; Liu et al., 2010; Qi et al., 2010). Both genes are associated with the positive regulation of gene expression and the removal of repressive marks. This raises the intriguing possibility that both enzymes might function in a linear pathway to sequentially demethylate H3K27me3 and thereby activate gene expression in response to mitochondrial perturbations. This hypothesis is supported by the mitochondrial stress-induced reduction of H3K27me3 occupancy at UPR^{mt} response genes during larval development in worms (Figure 7I). Our results are therefore consistent with the idea that removal of repressive

marks might allow access of the core UPR^{mt} transcriptional machinery to induce mitochondrial stress signaling (Haynes et al., 2010; Nargund et al., 2012).

How is mitochondrial stress sensed *by jmjd-1.2/PHF8* and *jmjd-3.1*/JMJD3? An attractive idea is that both *jmjd-1.2* and *jmjd-3.1* themselves are targets of the transcriptional response to mitochondrial stress as indicated in our transcriptomics analyses (Figure 5B). Another possibility is that acute adaptations in mitochondrial metabolism may promote activity of JmjC demethylases. Since both JMJD3 and PHF8 belong to the family of 2-oxoglutarate dependent oxygenases, it appears likely that elevated levels of the TCA cycle intermediate alpha-ketoglutarate (α-KG) might contribute to their increased activity (Teperino et al., 2010). Intriguingly, the exogenous supplementation of α-KG has recently been found to extend lifespan of *C. elegans* (Chin et al., 2014). While RNAi knockdown experiments for both *jmjd-1.2* and *jmjd-3.1* revealed robust suppression of ETC-mediated longevity and UPR^{mt} induction, we did not find strong effects on lifespan and *hsp-6* transcriptional induction in the analysis of the respective mutant strains suggesting that an acute depletion of the enzymes during larval development rather than chronic deficiency is necessary to unmask their role for these phenotypes (Figure S6).

In this work, we identify neurons as a key tissue to promote longevity and UPR^{mt} induction upon neuron-specific *jmjd-1.2* overexpression. Neuronal *jmjd-1.2* is not only sufficient to mediate a robust UPR^{mt} induction but also extends *C. elegans* lifespan in an UPR^{mt}-dependent manner. These findings were corroborated in mice and appear to be conserved in the BXD mouse reference population. Across various neuronal subregions, high levels of PHF8 and JMJD3 correlate with increased expression of mammalian UPR^{mt} core components (CLPP, ABCB10, SATB1/2, UBL5) and downstream mitochondrial chaperones HSP60 (HSPD1) and mtHSP70 (HSPA9) illustrating that both demethylases might control an integrated transcriptional network promoting mammalian longevity.

We previously demonstrated that mito-nuclear protein imbalance induces a robust UPR^{mt} and is linked to increased lifespan, both in nematodes and in BXD mice (Houtkooper et al., 2013). Interestingly, mito-nuclear imbalance might also play a role in longevity mediated by overexpression of *jmjd-1.2* and *jmjd-3.1*, as suggested by our RNA-seq analysis (Figure 5G). As further proof of concept that similar stressors could activate the UPR^{mt} across species, we recently found that expression of *Cox5b* and *Spg7* correlate negatively with the UPR^{mt} network, indicating that their low abundance likely triggers the UPR^{mt} in mammals (Wu et al., 2014). These data indicate that the UPR^{mt} pathway is active *in vivo* in mammals under physiological, non-stress conditions. Based on the observed positive correlations between PHF8, JMJD3 and UPR^{mt} in multiple tissues, we suggest that the regulation of UPR^{mt} by the H3K27 demethylases PHF8 and JMJD3 is also conserved in BXD mice under basal conditions. Of note, this association between histone demethylases and UPR^{mt} seems in certain tissues linked to mouse lifespan regulation, although further mechanistic work is required to ascertain this relation. Our bioinformatics analysis and literature discussed above suggests that PHF8 and JMJD3 regulate UPR^{mt} genes by removing repressive H3K27 methylation marks from their coding regions. Identifying the exact mechanism of regulation and whether there is a developmental aspect of the UPR^{mt} pathway in mammals, as

demonstrated in *C. elegans* (Durieux et al., 2011), remains an important direction for future work.

Collectively, our data corroborate the increasing body of literature in which epigenetic marks that control chromatin states, including histone methylation, represent a hallmark of aging (Greer et al., 2010; Han and Brunet, 2012; Lopez-Otin et al., 2013; Rando and Chang, 2012). Mitochondrial perturbations early in life have long-lasting effects on gene expression, and within this work we provide a mechanistic understanding of how this might be achieved. Our results thus reveal a conserved mode for the regulation of stress response and lifespan dependent on mitochondrial function.

Experimental Procedures

Additional details are provided in the Extended Experimental Procedures.

Lifespan Analysis

Lifespan experiments were conducted at 20°C as previously described (Durieux et al., 2011). Lifespans were performed on nematodes fed HT115 bacteria expressing the indicated RNAi, using the pre-fertile period of adulthood as day 0. Animals were transferred to fresh plates every other day until day 12. Prism 5 software was used for statistical analysis to determine significance calculated using the log-rank (Mantel-Cox) method. Lifespan experiments involving RNAi shifting to *Dicer (dcr-1)* RNAi were performed as described (Dillin et al., 2002a, 2002b). Briefly, for lifespans with selective RNAi only during development, animals were grown on *cco-1+jmjd-1.2* or *cco-1+jmjd-3.1* RNAi bacteria and transferred to *dcr-1* dsRNA expressing bacteria at L4 stage. For lifespans with RNAi during adulthood, animals were grown on empty vector RNAi control bacteria and transferred to *cco-1+jmjd-1.2* or *cco-1+jmjd-3.1* RNAi bacteria at L4 stage.

Gene Expression Analysis

C. elegans were age synchronized by egg bleaching and cultivated on nematode growth (NGM) plates containing HT115 bacteria expressing the indicated RNAi constructs at 20°C and harvested at day 1 of adulthood. Animals were collected in M9 buffer, centrifuged at 1000 × g for 30 sec, resuspended in Trizol (Life Technologies) and snap frozen in liquid nitrogen. After several freeze-thaw cycles, total RNA was isolated using the RNeasy Mini Kit (Qiagen) according to the manufacturer's instructions. 1 μg of total RNA was subjected to cDNA synthesis using the QuantiTect Reverse Transcription Kit (Qiagen). Quantitative Real-Time PCR reactions were performed with the SYBR Select Master Mix (Applied Biosystems) in Optical 384-well MicroAmp plates (Applied Biosystems) using a QuantStudio 6 Flex (Applied Biosystems).

Fluorescence Microscopy

For fluorescence microscopy, animals were blindly chosen under the light microscope (at random) from a population, immobilized with 100 μg/ml levamisole (Sigma) and images were then captured using a Leica M250FA automated fluorescent stereo microscope equipped with a Hamamatsu ORCA-ER camera.

Immunoblot Analysis

Mouse tissue extracts were prepared in modified RIPA buffer using a hand-held homogenizer (UltraTurrax). Crude lysates were centrifuged at 10,000 × g at 4°C for 10 min and total protein amount was determined with the DC Protein Assay (BioRad). Supernatants were supplemented with 4x SDS sample buffer, boiled for 5 min at 95°C and resolved by standard SDS-PAGE. Proteins were transferred to PVDF membranes (Immobilon). Equal loading was assessed with anti-β-actin (Abcam) antibodies.

Supplementary Material

Refer to Web version on PubMed Central for supplementary material.

Acknowledgments

We thank Dr. Y. Tian for help with reporter crosses, Lawrence Joe for preparing the RNA-seq libraries and Drs. C. Riera, P. Douglas and N. Baird for scientific insight. We thank Franziska Lorbeer for help with data analysis and Ed Ralston for help with gamma irradiation. We are grateful to Drs. A. Salcini, A. Carrano, M. Hansen, R. O'Sullivan and C. Holmberg for reagents. Some of the nematode strains used in this work were provided by the Japanese National BioResource Project and the CGC, which is supported by the NIH-Officer of Research Infrastructure Programs (P40 OD010440). This work used the Vincent J. Coates Genomics Sequencing Laboratory at UC Berkeley, supported by NIH S10 Instrumentation Grants S10RR029668 and S10RR027303. C.M. was supported by a postdoctoral fellowship from the Glenn Center for Aging Research at the Salk Institute for Biological Studies. S.D.J was supported by American Heart Association grant #15POST22510020. K.K.S. was supported by a grant from the Jane Coffin Childs Memorial Fund for Medical Research. This work was supported by the Howard Hughes Medical Institute (HHMI), NIH (R01 ES021667) to A.D., the Glenn Foundation for Medical Research to C.M. and S.C.W., the EPFL, NIH (R01AG043930), SwissCancerLeague (KFS-3082-02-2013), Systems X (SySX.ch 2013/153) and the SNSF (31003A-140780) to JA.

References

Agger K, Cloos PAC, Christensen J, Pasini D, Rose S, Rappsilber J, Issaeva I, Canaani E, Salcini AE, Helin K. UTX and JMJD3 are histone H3K27 demethylases involved in HOX gene regulation and development. Nature. 2007; 449:731–734. [PubMed: 17713478]

Andreux PA, Williams EG, Koutnikova H, Houtkooper RH, Champy MF, Henry H, Schoonjans K, Williams RW, Auwerx J. Systems genetics of metabolism: the use of the BXD murine reference panel for multiscalar integration of traits. Cell. 2012; 150:1287–1299. [PubMed: 22939713]

Baird NA, Douglas PM, Simic MS, Grant AR, Moresco JJ, Wolff SC, Yates JR 3rd, Manning G, Dillin A. HSF-1-mediated cytoskeletal integrity determines thermotolerance and life span. Science. 2014; 346:360–363. [PubMed: 25324391]

Baker MJ, Tatsuta T, Langer T. Quality control of mitochondrial proteostasis. Cold Spring Harb Perspect Biol. 2011; 3

Bender LB, Cao R, Zhang Y, Strome S. The MES-2/MES-3/MES-6 complex and regulation of histone H3 methylation in C. elegans. Curr Biol CB. 2004; 14:1639–1643. [PubMed: 15380065]

Benedetti C, Haynes CM, Yang Y, Harding HP, Ron D. Ubiquitin-like protein 5 positively regulates chaperone gene expression in the mitochondrial unfolded protein response. Genetics. 2006; 174:229–239. [PubMed: 16816413]

Chin RM, Fu X, Pai MY, Vergnes L, Hwang H, Deng G, Diep S, Lomenick B, Meli VS, Monsalve GC, et al. The metabolite α-ketoglutarate extends lifespan by inhibiting ATP synthase and TOR. Nature. 2014; 510:397–401. [PubMed: 24828042]

Copeland JM, Cho J, Lo T Jr, Hur JH, Bahadorani S, Arabyan T, Rabie J, Soh J, Walker DW. Extension of Drosophila life span by RNAi of the mitochondrial respiratory chain. Curr Biol. 2009; 19:1591–1598. [PubMed: 19747824]

Dell'agnello C, Leo S, Agostino A, Szabadkai G, Tiveron C, Zulian A, Prelle A, Roubertoux P, Rizzuto R, Zeviani M. Increased longevity and refractoriness to Ca(2+)-dependent neurodegeneration in Surf1 knockout mice. Hum Mol Genet. 2007; 16:431–444. [PubMed: 17210671]

Dillin A, Hsu AL, Arantes-Oliveira N, Lehrer-Graiwer J, Hsin H, Fraser AG, Kamath RS, Ahringer J, Kenyon C. Rates of behavior and aging specified by mitochondrial function during development. Science. 2002a; 298:2398–2401. [PubMed: 12471266]

Dillin A, Crawford DK, Kenyon C. Timing requirements for insulin/IGF-1 signaling in C. elegans. Science. 2002b; 298:830–834. [PubMed: 12399591]

Durieux J, Wolff S, Dillin A. The cell-non-autonomous nature of electron transport chain-mediated longevity. Cell. 2011; 144:79–91. [PubMed: 21215371]

Feng J, Bussiere F, Hekimi S. Mitochondrial electron transport is a key determinant of life span in Caenorhabditis elegans. Dev Cell. 2001; 1:633–644. [PubMed: 11709184]

Feng W, Yonezawa M, Ye J, Jenuwein T, Grummt I. PHF8 activates transcription of rRNA genes through H3K4me3 binding and H3K9me1/2 demethylation. Nat Struct Mol Biol. 2010; 17:445–450. [PubMed: 20208542]

Fortschegger K, de Graaf P, Outchkourov NS, van Schaik FMA, Timmers HTM, Shiekhattar R. PHF8 targets histone methylation and RNA polymerase II to activate transcription. Mol Cell Biol. 2010; 30:3286–3298. [PubMed: 20421419]

Greer EL, Maures TJ, Hauswirth AG, Green EM, Leeman DS, Maro GS, Han S, Banko MR, Gozani O, Brunet A. Members of the H3K4 trimethylation complex regulate lifespan in a germline-dependent manner in C. elegans. Nature. 2010; 466:383–387. [PubMed: 20555324]

Han S, Brunet A. Histone methylation makes its mark on longevity. Trends Cell Biol. 2012; 22:42–49. [PubMed: 22177962]

Haynes CM, Petrova K, Benedetti C, Yang Y, Ron D. ClpP mediates activation of a mitochondrial unfolded protein response in C. elegans. Dev Cell. 2007; 13:467–480. [PubMed: 17925224]

Haynes CM, Yang Y, Blais SP, Neubert TA, Ron D. The matrix peptide exporter HAF-1 signals a mitochondrial UPR by activating the transcription factor ZC376.7 in C. elegans. Mol Cell. 2010; 37:529–540. [PubMed: 20188671]

Heinemann B, Nielsen JM, Hudlebusch HR, Lees MJ, Larsen DV, Boesen T, Labelle M, Gerlach LO, Birk P, Helin K. Inhibition of demethylases by GSK-J1/J4. Nature. 2014; 514:E1–E2. [PubMed: 25279926]

Houtkooper RH, Mouchiroud L, Ryu D, Moullan N, Katsyuba E, Knott G, Williams RW, Auwerx J. Mitonuclear protein imbalance as a conserved longevity mechanism. Nature. 2013; 497:451–457. [PubMed: 23698443]

Hsin H, Kenyon C. Signals from the reproductive system regulate the lifespan of C. elegans. Nature. 1999; 399:362–366. [PubMed: 10360574]

Huang DW, Sherman BT, Lempicki RA. Systematic and integrative analysis of large gene lists using DAVID bioinformatics resources. Nat Protoc. 2009; 4:44–57. [PubMed: 19131956]

Kenyon C, Chang J, Gensch E, Rudner A, Tabtiang R. A C. elegans mutant that lives twice as long as wild type. Nature. 1993; 366:461–464. [PubMed: 8247153]

Kirchman PA, Kim S, Lai CY, Jazwinski SM. Interorganelle signaling is a determinant of longevity in Saccharomyces cerevisiae. Genetics. 1999; 152:179–190. [PubMed: 10224252]

Kirkwood TB. Understanding the odd science of aging. Cell. 2005; 120:437–447. [PubMed: 15734677]

Kleine-Kohlbrecher D, Christensen J, Vandamme J, Abarrategui I, Bak M, Tommerup N, Shi X, Gozani O, Rappsilber J, Salcini AE, et al. A functional link between the histone demethylase PHF8 and the transcription factor ZNF711 in X-linked mental retardation. Mol Cell. 2010; 38:165–178. [PubMed: 20346720]

Kooistra SM, Helin K. Molecular mechanisms and potential functions of histone demethylases. Nat Rev Mol Cell Biol. 2012; 13:297–311. [PubMed: 22473470]

Labbadia J, Morimoto RI. Repression of the Heat Shock Response Is a Programmed Event at the Onset of Reproduction. Mol Cell. 2015; 59:639–650. [PubMed: 26212459]

Lakowski B, Hekimi S. The genetics of caloric restriction in Caenorhabditis elegans. Proc Natl Acad Sci U S A. 1998; 95:13091–13096. [PubMed: 9789046]

Lee SS, Lee RY, Fraser AG, Kamath RS, Ahringer J, Ruvkun G. A systematic RNAi screen identifies a critical role for mitochondria in C. elegans longevity. Nat Genet. 2003; 33:40–48. [PubMed: 12447374]

Liu W, Tanasa B, Tyurina OV, Zhou TY, Gassmann R, Liu WT, Ohgi KA, Benner C, Garcia-Bassets I, Aggarwal AK, et al. PHF8 mediates histone H4 lysine 20 demethylation events involved in cell cycle progression. Nature. 2010; 466:508–512. [PubMed: 20622854]

Liu X, Jiang N, Hughes B, Bigras E, Shoubridge E, Hekimi S. Evolutionary conservation of the clk-1-dependent mechanism of longevity: loss of mclk1 increases cellular fitness and lifespan in mice. Genes Dev. 2005; 19:2424–2434. [PubMed: 16195414]

Lopez-Otin C, Blasco MA, Partridge L, Serrano M, Kroemer G. The hallmarks of aging. Cell. 2013; 153:1194–1217. [PubMed: 23746838]

Morimoto RI. The heat shock response systems biology of proteotoxic stress in aging and disease. Cold Spring Harb Symp Quant Biol. 2011; 76:91–99. [PubMed: 22371371]

Nargund AM, Pellegrino MW, Fiorese CJ, Baker BM, Haynes CM. Mitochondrial import efficiency of ATFS-1 regulates mitochondrial UPR activation. Science. 2012; 337:587–590. [PubMed: 22700657]

Nargund AM, Fiorese CJ, Pellegrino MW, Deng P, Haynes CM. Mitochondrial and nuclear accumulation of the transcription factor ATFS-1 promotes OXPHOS recovery during the UPR(mt). Mol Cell. 2015; 58:123–133. [PubMed: 25773600]

Ntziachristos P, Tsirigos A, Welstead GG, Trimarchi T, Bakogianni S, Xu L, Loizou E, Holmfeldt L, Strikoudis A, King B, et al. Contrasting roles of histone 3 lysine 27 demethylases in acute lymphoblastic leukaemia. Nature. 2014; 514:513–517. [PubMed: 25132549]

Owusu-Ansah E, Song W, Perrimon N. Muscle mitohormesis promotes longevity via systemic repression of insulin signaling. Cell. 2013; 155:699–712. [PubMed: 24243023]

Qi HH, Sarkissian M, Hu GQ, Wang Z, Bhattacharjee A, Gordon DB, Gonzales M, Lan F, Ongusaha PP, Huarte M, et al. Histone H4K20/H3K9 demethylase PHF8 regulates zebrafish brain and craniofacial development. Nature. 2010; 466:503–507. [PubMed: 20622853]

Rando TA, Chang HY. Aging, rejuvenation, and epigenetic reprogramming: resetting the aging clock. Cell. 2012; 148:46–57. [PubMed: 22265401]

Rea SL, Ventura N, Johnson TE. Relationship between mitochondrial electron transport chain dysfunction, development, and life extension in Caenorhabditis elegans. PLoS Biol. 2007; 5:e259. [PubMed: 17914900]

Schon EA, Przedborski S. Mitochondria: the next (neurode)generation. Neuron. 2011; 70:1033–1053. [PubMed: 21689593]

Schroeder EA, Raimundo N, Shadel GS. Epigenetic silencing mediates mitochondria stress-induced longevity. Cell Metab. 2013; 17:954–964. [PubMed: 23747251]

Taylor RC, Dillin A. XBP-1 Is a Cell-Nonautonomous Regulator of Stress Resistance and Longevity. Cell. 2013; 153:1435–1447. [PubMed: 23791175]

Teperino R, Schoonjans K, Auwerx J. Histone methyl transferases and demethylases; can they link metabolism and transcription? Cell Metab. 2010; 12:321–327. [PubMed: 20889125]

Tsang WY, Lemire BD. Mitochondrial genome content is regulated during nematode development. Biochem Biophys Res Commun. 2002; 291:8–16. [PubMed: 11829454]

Walter P, Ron D. The unfolded protein response: from stress pathway to homeostatic regulation. Science. 2011; 334:1081–1086. [PubMed: 22116877]

Wu Y, Williams EG, Dubuis S, Mottis A, Jovaisaite V, Houten SM, Argmann CA, Faridi P, Wolski W, Kutalik Z, et al. Multilayered genetic and omics dissection of mitochondrial activity in a mouse reference population. Cell. 2014; 158:1415–1430. [PubMed: 25215496]

Yoneda T, Benedetti C, Urano F, Clark SG, Harding HP, Ron D. Compartment-specific perturbation of protein handling activates genes encoding mitochondrial chaperones. J Cell Sci. 2004; 117:4055–4066. [PubMed: 15280428]

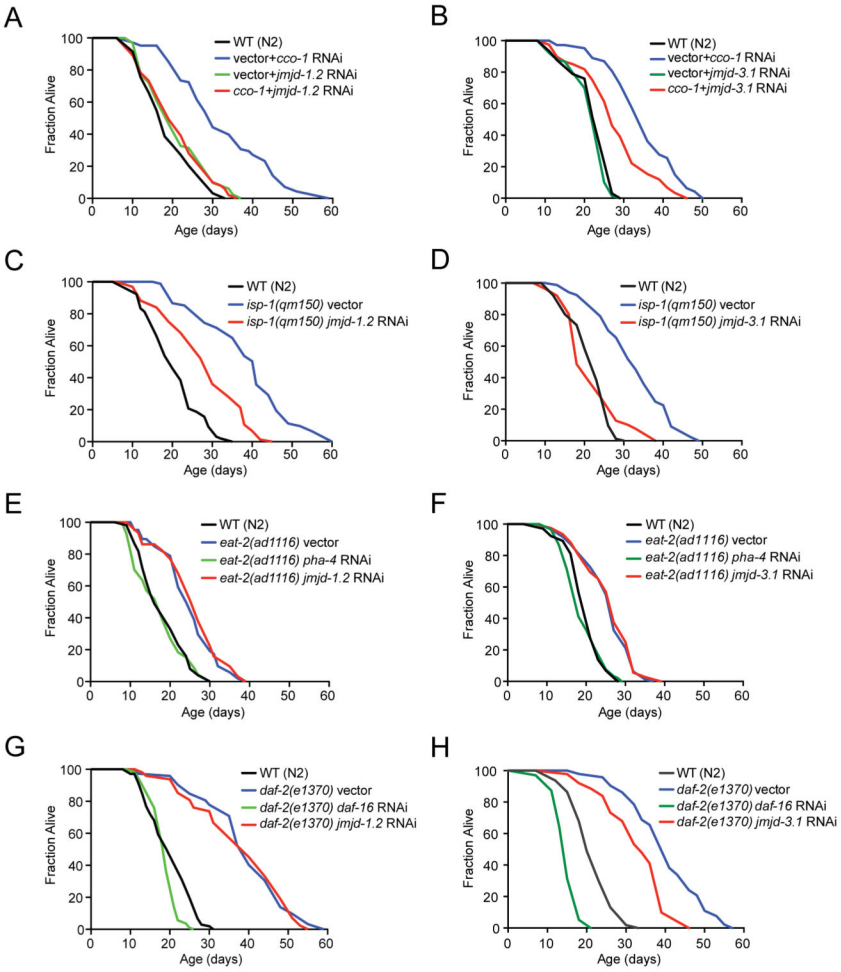

Figure 1. Lifespan Extension by Mitochondrial ETC Perturbation Requires the Histone Demethylases *jmjd-1.2* and *jmjd-3.1*

(A) and (B) Knockdown of *jmjd-1.2* (A) or *jmjd-3.1* (B) suppresses *cco-1*-mediated lifespan extension.

(C) *jmjd-1.2* is partially required for longevity of *isp-1(qm150)* mutant animals.

(D) *jmjd-3.1* is required for longevity of *isp-1(qm150)* mutant animals.

(E) and (F) Dietary restriction-mediated longevity of *eat-2(ad1116)* animals is not affected by *jmjd-1.2* (E) or *jmjd-3.1* (F) knockdown.

(G) Longevity of *daf-2(e1370)* mutant animals is not affected by *jmjd-1.2* knockdown.

(H) Longevity of *daf-2(e1370)* mutant animals partially depends on *jmjd-3.1*. See also Figure S1 and Table S1 for lifespan statistics.

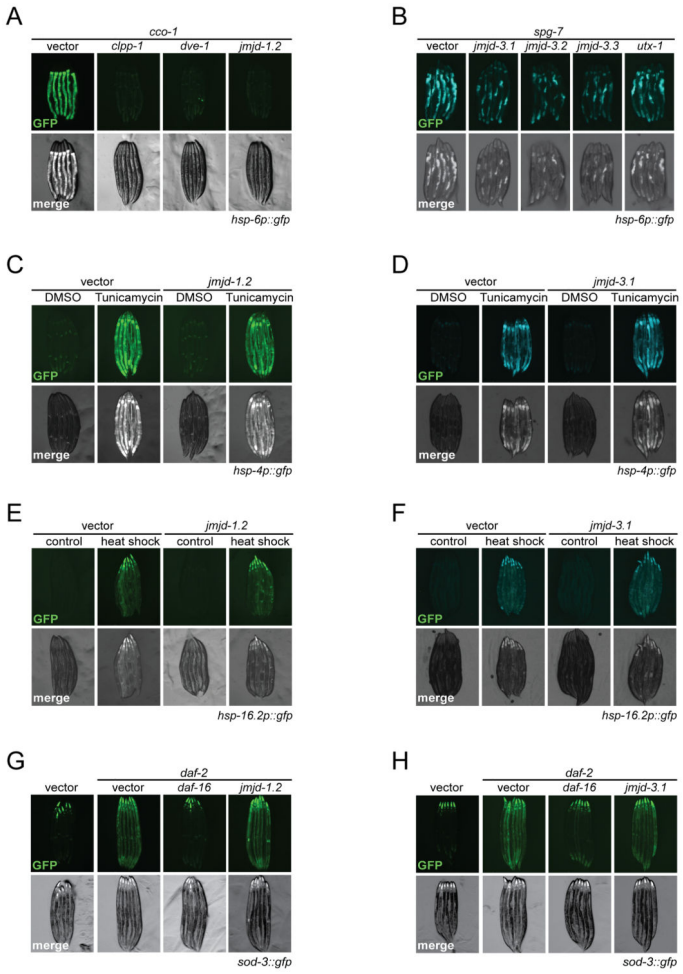

Figure 2. *jmjd-1.2* and *jmjd-3.1* are Necessary and Specific for Induction of the UPR^{mt}

(A) Fluorescent micrographs of *hsp-6p: :gfp* UPR^{mt} reporter animals treated with the indicated RNAi at day 1 of adulthood. Knockdown of *jmjd-1.2* suppresses *cco-1*-mediated UPR^{mt} induction in *hsp-6p: :gfp* reporter animals.

(B) Knockdown of *jmjd-3* histone demethylase family members suppresses *spg-7*-mediated UPR^{mt} induction.

(C) and (D) Fluorescent micrographs of *hsp-4p: :gfp* UPR^{er} reporter animals. Induction of the UPR^{er} response in *hsp-4p: :gfp* UPR^{er} reporter animals by tunicamycin treatment is not affected by neither *jmjd-1.2* (C) or *jmjd-3.1* (D) RNAi.

(E) and (F) Fluorescent micrographs of *hsp-16.2p: :gfp* reporter animals. Induction of the heat shock response in *hsp-16.2p: :gfp* reporter animals occurs independently of *jmjd-1.2* (E) or *jmjd-3.1* (F) RNAi.

(G) and (H) Fluorescent micrographs of *sod-3: :gfp* reporter animals treated with the indicated RNAi. *daf-16* RNAi was used as a positive control. See also Figures S2 and S3.

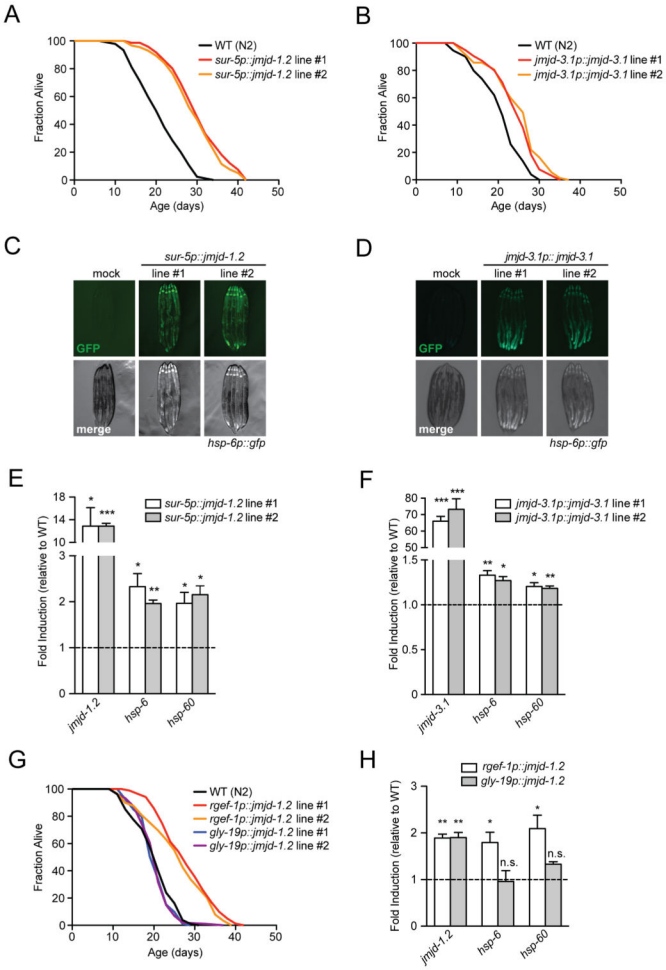

Figure 3. *jmjd-1.2* and *jmjd-3.1* Overexpression is Sufficient for Lifespan Extension and UPR^{mt} Induction

(A) and (B) Overexpression of *jmjd-1.2* and *jmjd-3.1* extends *C. elegans* lifespan. Lifespan analysis of two independent transgenic lines of *sur-5p.::jmjd-1.2* (A) or *jmjd-3.1p.::jmjd-3.1* (B) expressing animals compared to WT (N2) animals.

(C) and (D) Fluorescent micrographs of *hsp-6p.::gfp* UPR^{mt} reporter animals expressing either *sur-5p.::jmjd-1.2* (C) or *jmjd-3.1p.::jmjd-3.1* (D) transgenes in two independent lines analyzed at day 1 of adulthood.

(E) and (F) Transcript levels in two independent lines of *sur-5p.::jmjd-1.2* (E) or *jmjd-3.1p.::jmjd-3.1* (F) expressing animals at day 1 of adulthood were measured by qRT-PCR. Results are shown relative to transcript levels in WT (N2) animals, with error bars indicating mean ± SEM. *** denotes $p < 0.001$, **$p < 0.01$, *$p < 0.05$.

(G) Neuron-specific overexpression of *jmjd-1.2* is sufficient to extend lifespan. Lifespan analysis of two independent lines expressing either pan-neuronal (*rgef-1p.::jmjd-1.2) or intestinal (gly-19p.::jmjd-1.2)* transgenes compared to WT (N2) animals.

(H) Transcript levels in animals expressing either pan-neuronal (*rgef-1p.::jmjd-1.2)* or intestinal *(gly-19p.::jmjd-1.2)* transgenes at day 1 of adulthood were measured by qRT-PCR. Results are shown relative to transcript levels in WT (N2) animals, with error bars indicating

mean ± SEM. ** denotes $p < 0.01$, *$p < 0.05$, n.s. = $p > 0.05$. See also Figure S4 and Table S1 for lifespan statistics.

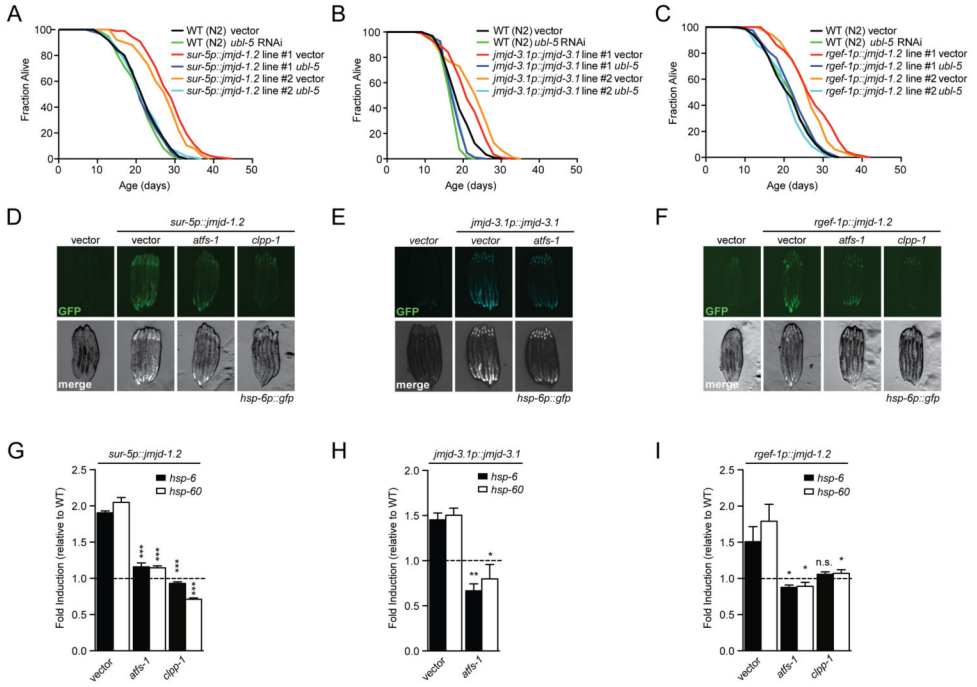

Figure 4. The UPR^{mt} is a Genetic Requirement for the Pro-Longevity Response upon *jmjd-1.2* and *jmjd-3.1* Overexpression

(A), (B) and (C) *ubl-5* RNAi suppresses lifespan extension upon *jmjd-1.2*, *jmjd-3.1* or neuronal *jmjd-1.2* overexpression. Lifespan analysis of two independent lines of *sur-5p*::*jmjd-1.2* (A), *jmjd-3.1p*::*jmjd-3.1* (B), neuronal *rgef-1p*::*jmjd-1.2* (C) and WT (N2) animals grown on empty vector control or *ubl-5* RNAi.

(D), (E) and (F) Fluorescent micrographs of *hsp-6p*::*gfp* UPR^{mt} reporter animals expressing the indicated transgenes treated with the indicated RNAi, at day 1 of adulthood.

(G), (H) and (I) Transcript levels of canonical UPR^{mt} targets assessed by qRT-PCR in *sur-5p*::*jmjd-1.2* (G), *jmjd-3.1p*::*jmjd-3.1* (H) or neuronal *rgef-1p*::*jmjd-1.2* (I) transgenic animals at day 1 of adulthood treated with the indicated RNAi. Results are shown relative to transcript levels in WT (N2) animals grown on the indicated RNAi, with error bars indicating mean ± SEM. *** denotes $p < 0.001$, **$p < 0.01$, *$p < 0.05$, n.s. = $p > 0.05$. See also Figure S5 and Table S1 for lifespan statistics.

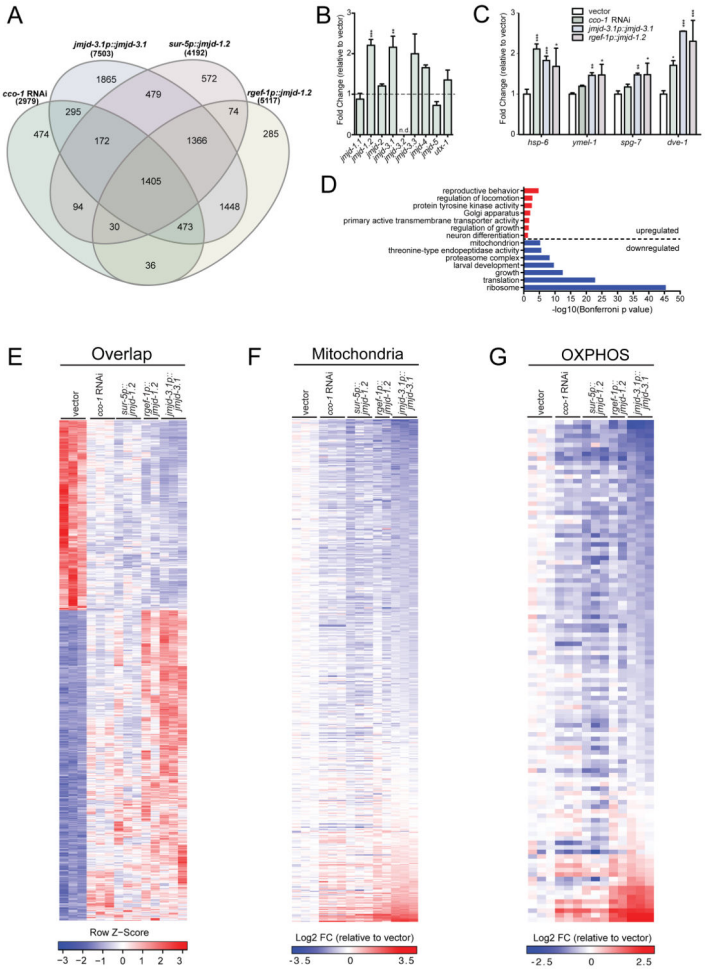

Figure 5. ETC Perturbation and JMJD Overexpression Share Common Lifespan Extension Mechanisms

(A) Venn diagram of differentially expressed genes (DEGs) in *cco-1* RNAi treated worms and transgenic overexpression lines *jmjd-3.1p*: :*jmjd-3.1*, *sur-5p*: :*jmjd-1.2*, *rgef-1p*: :*jmjd-1.2*, compared to wild type N2 worms on empty vector control, as measured by RNA-seq (Benjamini-Hochberg adjusted p value < 0.05). See Table S2 for complete list of DEGs.

(B) Transcriptional upregulation of *jmjd-1.2* and *jmjd-3.1* upon *cco-1* RNAi. Gene expression analysis of all nine JmjC domain encoding genes in RNA-seq samples, expressed as fold change relative to wild type N2 on empty vector control. Results are expressed as mean ±SEM of normalized count values (n=3, Benjamini-Hochberg adjusted p values (padj) calculated by DESeq2, *jmjd-1.2* padj=6.93E-09, *jmjd-3.1* padj=0.002, *jmjd-3.3* padj=0.452, *jmjd-4* padj=0.085. n.d.= not detected, ** denotes p < 0.01, ***p < 0.001).

(C) UPR^{mt} gene expression in RNA-seq samples, expressed as fold change relative to wild type N2 on empty vector control. Results are expressed as mean ±SEM of normalized count values. * denotes p < 0.05, **p < 0.01, ***p < 0.001).

(D) Representative top GO terms of upregulated and downregulated genes in the 1405 overlapping DEGs (Bonferroni adjusted p value<0.05). See also Table S2.

(E) Gene expression heatmap of 1405 overlapping DEGs in all 4 conditions described in(A). DESeq2-normalized count values were used for calculations. The indicated Row Z-scores reflect the number of standard deviations each replicate is apart from the mean gene expression value over all conditions. See also Table S2.
(F) Heatmap of 470 mitochondrial genes from GO cellular component category mitochondrion (GO:0005739). Fold change (FC) was calculated by comparing normalized count values of each condition to wild type N2 empty vector control, then transformed to log2 scale. See also Table S2.
(G) Heatmap of 111 OXPHOS genes from GO biological process category oxidative phosphorylation (GO:0006119) and manual annotation. See also Table S2.

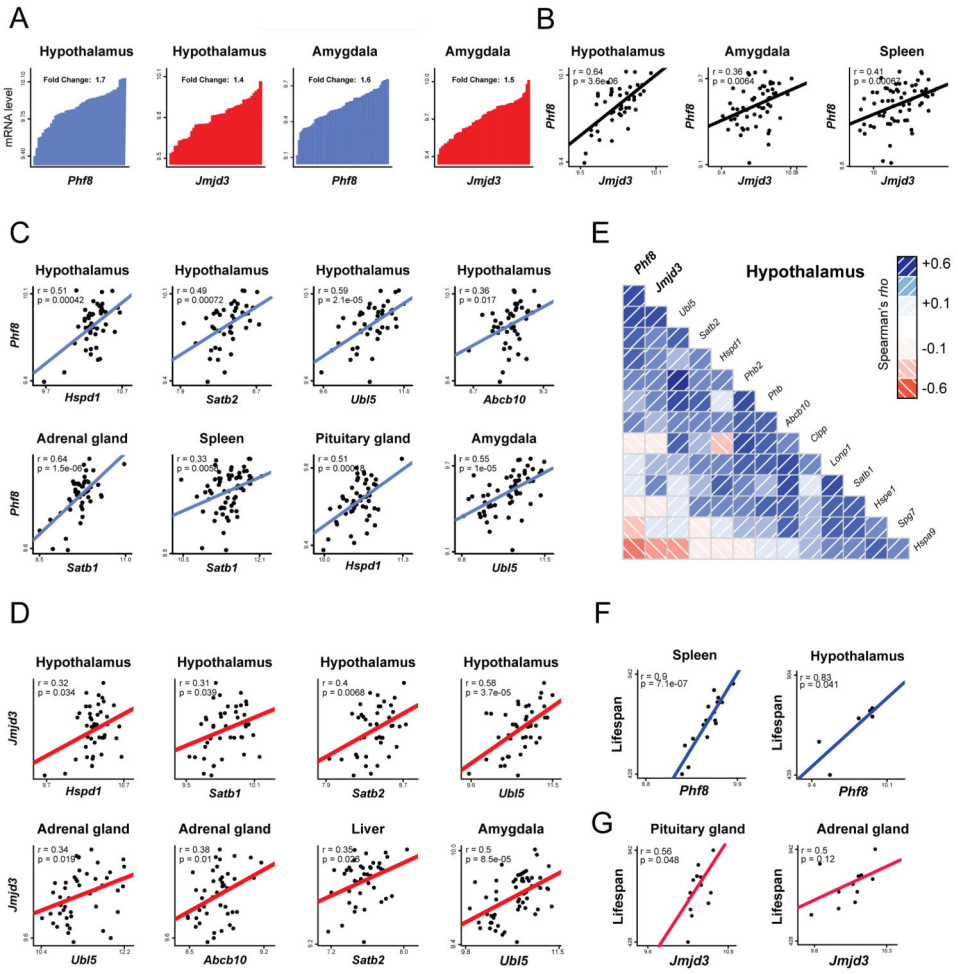

Figure 6. Positive Correlations between *Phf8*, *Jmjd3*, Lifespan and UPR^{mt} transcripts in the BXD Mouse Genetic Reference Population

(A) Variation of *Phf8* and *Jmjd3* mRNA levels in hypothalamus (n=44) and amygdala(n=56) across BXD mouse strains. Each bar represents mRNA levels from a pool of approximately five animals per strain.

(B) Positive correlations between *Phf8* (y-axis) and *Jmjd3* (x-axis) expression in hypothalamus (n=44), amygdala (n=56) and spleen (n=67).

(C) Positive correlations between *Phf8* (y-axis) and selected UPR^{mt} genes (x-axis) transcripts in various tissues (n=46 for adrenal gland, n=49 for pituitary gland).

(D) Positive correlations between *Jmjd3* (y-axis) and selected UPR^{mt} genes (x-axis) transcripts in various tissues (n=46 for liver).

(E) Spearman's correlation co-expression network for *Phf8*, *Jmjd3* and UPR^{mt} genes in hypothalamus. Blue correlations are positive, red correlations are negative – intensity of the colors corresponds to correlation coefficients.

(F) Pearson correlations of Lifespan versus *Phf8* transcript levels in either spleen (left) or hypothalamus (right) of BXD mice.

(G) Pearson correlations of Lifespan versus *Jmjd3* transcript levels in either pituitarygl and (left) or adrenal gland (right) of BXD mice.

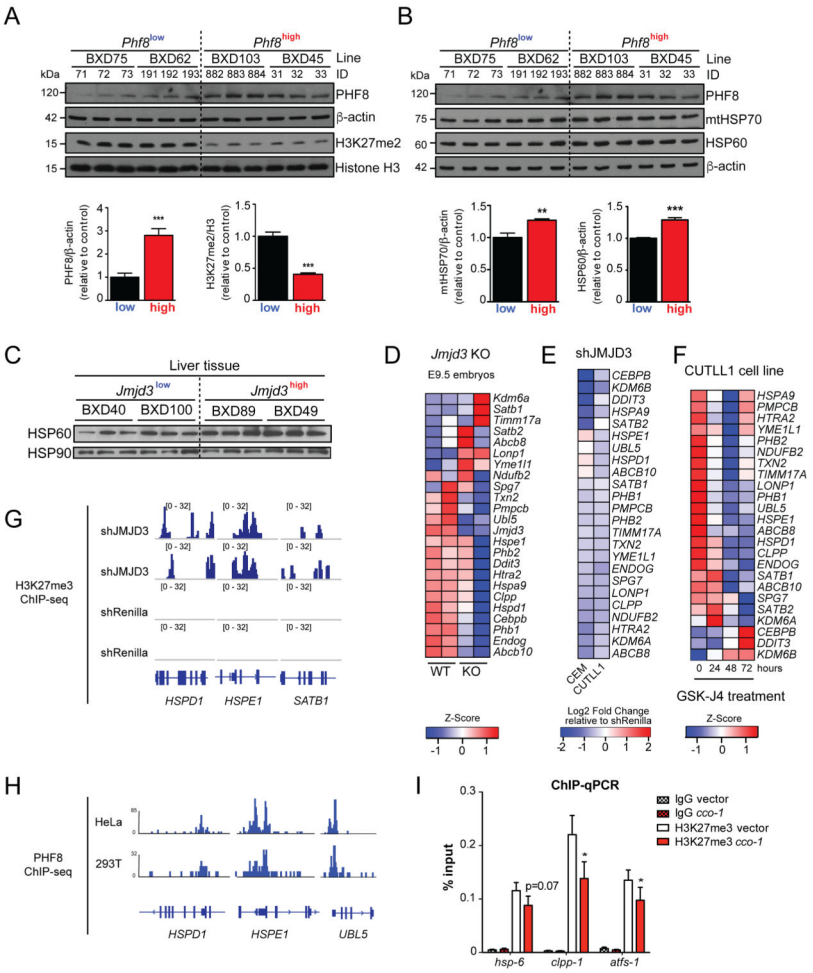

Figure 7. Conserved UPR^{mt} Gene Regulation Mechanisms Through H3K27 Demethylases

(A) and (B) Immunoblot analysis of tissue protein lysates using the indicated antibodies. Increased *Phf8* expression correlates with reduced H3K27me2 (A) and higher levels of mitochondrial chaperones (B) in the hypothalamus of the indicated BXD mouse strains. β-actin and Histone H3 were used as loading controls (upper panels). Densitometric quantifications of immunoblot signals normalized to either β-actin or Histone H3 (lower panels). Data represent the mean+ SEM. *** denotes $p < 0.001$, **$p < 0.01$.

(C) Immunoblot analysis of BXD liver tissue protein lysates using the indicated antibodies. HSP90 was used as a loading control.

(D) Heatmap of selected UPR^{mt} transcripts in WT and *Jmjd3* KO mice embryos at E9.5 (GSE40332). Low expression is shown in blue, while high expression is in red.

(E) Heatmap of fold change in UPR^{mt} transcripts upon shJMJD3 treatment relative to shRenilla in human T-cell lymphoblastic leukemia CEM and CUTLL1 cell lines (GSE56696).

(F) Heatmap of selected UPR^{mt} transcripts in the human T-cell lymphoblastic leukemia CUTLL1 cell line upon treatment with the H3K27 demethylase inhibitor GSK-J4 (GSE56696).

(G) ChIP-Seq profiles of H3K27me3 enrichment at selected UPR^{mt} genes in the CUTLL1 cell line upon shJMJD3 and shRenilla treatments (GSE56696).
(H) ChIP-Seq profiles of PHF8 binding at selected UPR^{mt} gene promoters in HeLa and 293T cells (GSE20725).
(I) ChIP-qRT-PCR analysis of H3K27me3 enrichment at UPR^{mt} genes at L3 stage of *cco-1* RNAi treated worms compared to empty vector control. IgG antibody was used as a control. Results are expressed as percent of input, with error bars indicating mean ± SEM (n=7, * denotes $p < 0.01$).